The charge carrier localization in the cubic perovskite $BaOsO_3$ revealed by an optical study

2014 J. Phys.: Condens. Matter 26 435601

(http://iopscience.iop.org/0953-8984/26/43/435601)

IOP Publishing Journal of Physics: Condensed Matter

J. Phys.: Condens. Matter **26** (2014) 435601 (5pp) doi:10.1088/0953-8984/26/43/435601

The charge carrier localization in the cubic perovskite $BaOsO_3$ revealed by an optical study

P Zheng[1], Y G Shi[1], A F Fang[1], T Dong[1], K Yamaura[2] and N L Wang[1,3]

[1] Beijing National Laboratory for Condensed Matter Physics, Institute of Physics, Chinese Academy of Sciences, Beijing 100190, People's Republic of China
[2] Superconducting Properties Unit, National Institute for Materials Science, 1-1 Namiki, Tsukuba, 305-0044 Ibaraki, Japan
[3] International Center for Quantum Materials, School of Physics, Peking University, Beijing 100871, People's Republic of China

E-mail: pzheng@aphy.iphy.ac.cn

Received 6 June 2014, revised 19 August 2014
Accepted for publication 9 September 2014
Published 9 October 2014

Abstract

We present the optical conductivity spectra for the newly discovered cubic perovskite structure $BaOsO_3$ at various temperatures. The compound exhibits metallic behaviour above 50 K, but becomes non-metallic below 50 K. However, below 550 cm^{-1}, neither the typical Drude response nor an energy gap is observed in optical conductivity spectra from 300 K to 10 K. A broad peak centred at about 550 cm^{-1} is observed in the real part of optical conductivity $\sigma_1(\omega)$. The structure could be well reproduced by the localization modified Drude model. The life time of the carrier, deduced from $\sigma_1(\omega)$ in terms of the localization modified Drude model, decreases with T varying from 300 K to 100 K, then increases slightly at 10 K. The study indicates that the compound is at the boundary of metal-insulator transition.

Keywords: metal-insulator transition, transition-metal compounds, infrared spectra, localization, correlated electrons

(Some figures may appear in colour only in the online journal)

1. Introduction

Metal-insulator transition (MIT) is one of the important phenomena in condensed matter physics and has attracted much attention. In recent years, some partially filled 5d transition metal oxides, such as Sr_2IrO_4 [1–3], $Cd_2Os_2O_7$ [4], $Ca_2Os_2O_7$ [5], Ca_3LiOsO_6 [6], $NaIrO_3$ [7] *et al*, were found to be abnormally insulating at low temperature, which stimulated many experimental and theoretical studies [1–5, 8]. 4d and 5d transition metal oxides were considered as weakly correlated wide band systems, in which the on-site Coulomb repulsive interaction is largely reduced due to delocalized 4d and 5d states [1, 3, 9]. Simultaneously, as the atomic mass increases, the spin-orbital coupling (SOC) becomes more and more important, which also plays an essential role in 4d/5d materials. With these two effects, the electronic properties of 4d/5d metal oxides become more complex and abundant and many new physical phenomena emerge. The novel insulator state is first observed in Sr_2IrO_4 with five electrons filling the Ir 5d t_{2g} band [1–3]. In this system, strong SOC splits the Ir 5d t_{2g} band into two groups of bands with effective total angular momentum $j = 1/2$ and $j = 3/2$ respectively. The $j = 3/2$ bands are nearly fully filled while the $j = 1/2$ bands are half filled. Such a system could be simplified to an effective one-band half-filled system with a narrowed bandwidth. The on-site Coulomb interaction splits the half-filled degenerate bands into empty upper Hubbard bands and full-filled lower Hubbard bands, resulting in a Mott insulator state. However in the post perovskite structure of paramagnetic insulator $NaIrO_3$ [10–12] with four electrons filling the Ir 5d t_{2g} band, it is found that the SOC split is smaller than the t_{2g} band. As a result, SOC alone could not generate an insulator in this system. This is in contrast to the experimental observation. Then a newly developed local density approximation plus the Gutzwiller

method is used in theoretical calculation based on the multi-band Hubbard model [10–12]. The calculation reveals that the cooperation of a finite Coulomb interaction and SOC tends to favour the re-normalized band insulator of $NaIrO_3$ [10–12]. The study of the partially filled t_{2g} enriches the Mott metal-insulator transition theory.

The perovskite $BaOsO_3$ is a new Osmium oxide. Its crystal structure is cubic perovskite with the space group $Pm\bar{3}m(2\,2\,1)$ [6]. The OsO_6 octahedras are corner-sharing and compose a three dimensional cubic network. Here Os 5d t_{2g} bands are filled with four electrons because the $BaOsO_3$ adopts the octahedral environment of OsO_6 with $5d^4$ configuration. It is reported that the compound exhibits enhanced paramagnetism to 2 K [6]. A relatively high Sommerfeld coefficient of 16.8(1) mJ mol^{-1} K^{-2} could be deduced from the specific heat data. The temperature dependence of the resistivity ρ (T) is a metallic type above 60 K, while it turns up below 40 K and clearly shows a minus temperature dependence. The first-principles calculations taking into consideration the SOC, proposed a nonzero electronic DOS at the E_F level [6, 13]. The mechanism of the change of the electric conducting behavior is not clear. Interestingly, $BaOsO_3$ and $NaIrO_3$ have two similar features: (1) The 5d t_{2g} bands are filled with four electrons. (2) The SOC split is smaller than the t_{2g} band and so could not generate an insulator with a direct energy gap by itself. Detecting the electronic structure of $BaOsO_3$ is one of the important experiments. Optical spectroscopy is a powerful tool to probe the electronic structure and charge dynamics. In this paper, we performed the optical reflectivity measurement. No energy gap was observed in the far infrared frequency region from 300 K to 10 K. A characteristic broad peak appears in the far-infrared frequency regime at all temperatures. As the temperature decreases, the spectra weights redistribute in a wide energy scale. Our study reveals the correlated localization characters of $BaOsO_3$.

2. Experiments

To date, single crystals are not available for cubic perovskite $BaOsO_3$. Polycrystal samples could be prepared only under high pressure conditions [6]. The *dc* resistivity (ρ(T)) (figure 1) was carried out with a four-probes method on a Quantum Design physical property measurement system (PPMS). Since $BaOsO_3$ is of cubic crystal structure without anisotropy, the polycrystalline is suitable for the optical measurement. According to [6], the crystal structure parameter is $a = 4.02573$ Å, then the ideal density of the material should be 9.558 g cm^{-3}. After measuring the size of our sample and weight, we found the mass density of the polycrystallite to be roughly 8.66 g cm^{-3}. The sample in our experiment is of rather high density after the 17 GPa high pressure preparation. The sample surface was carefully polished for optical measurement. The optical reflectivity R(w) was measured from 30 cm^{-1} to 25 000 cm^{-1} at different temperatures on a Fourier transform spectrometer (Bruker 80 v). The frequency-dependent optical conductivity and dielectric constant are derived from Kramers–Kronig

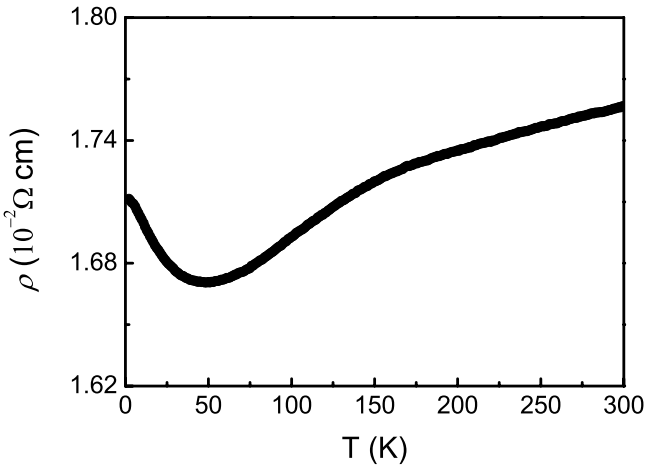

Figure 1. The temperature dependence of resistivity.

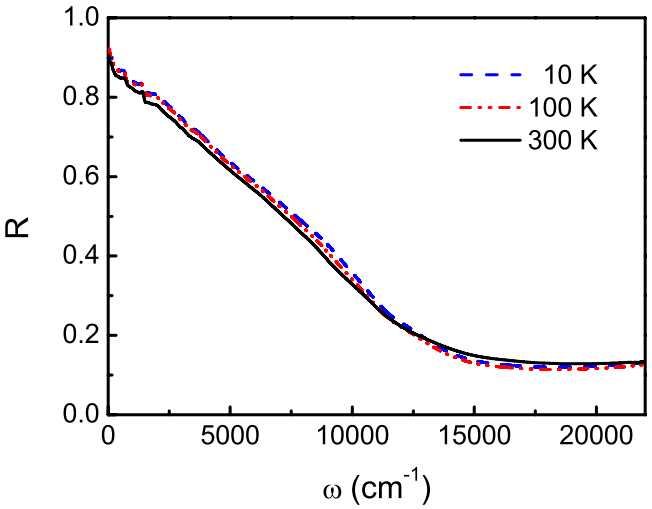

Figure 2. The frequency dependence of reflectivity R (ω) at 10 K, 100 K and 300 K, respectively.

transformations. We used Hagen–Rubens relation for low frequency extrapolations. We found that different low frequency extrapolations do not affect the conductivity spectra in the measured frequency region. In the high energy side, the measured reflectivity curve is extrapolated constantly to 100 000 cm^{-1}, above which a well-known function of ω^{-4} is used.

3. Results and discussions

Figure 2 shows the reflectivity spectra (R(ω)) from 30 cm^{-1} to 22 000 cm^{-1} at various temperatures. The reflectivity monotonically decreases with the frequency ω increasing up to 15 000 cm^{-1} at three different temperatures. Such a near linear frequency dependence of R throughout the infrared region is similar to that of cuprates in which the carriers are overdamped [14]. Above 15 000 cm^{-1} R(ω) is weakly ω-dependent. R(ω) slightly but obviously varies with temperature in a large frequency regime. Figure 3 is a collection of the real part of the optical conductivity $\sigma_1(\omega)$ at 10 K, 100 K and 300 K, respectively. All the conductivity

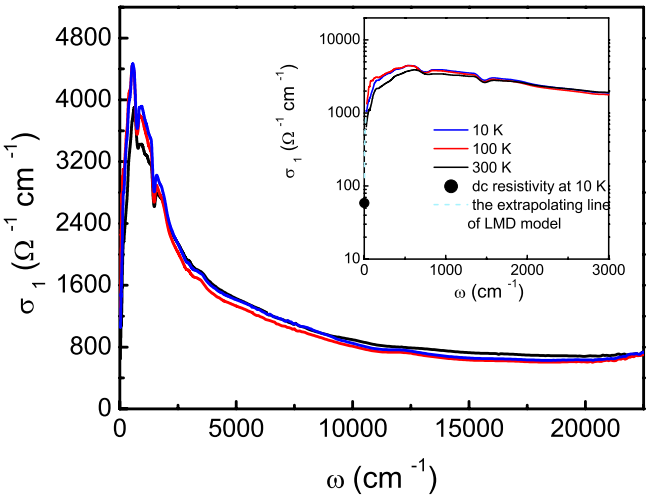

Figure 3. The frequency dependence of the optical conductivity at 10 K, 100 K and 300 K. The inset is the enlarged plot of $\sigma_1(\omega)$. The dot is the *dc* conductivity at 10 K. The dashed–dot line is the fitting results of the localization modified Drude model.

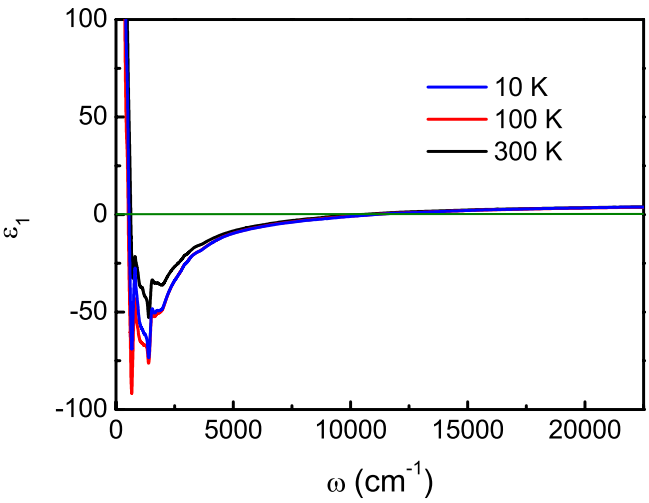

Figure 4. The frequency dependence of the real part of the dielectric constant. The solid line is for $\epsilon_1 = 0$.

spectra at different temperatures show a broad peak centred at about 550 cm^{-1} (about 0.07 eV). Below 550 cm^{-1}, σ_1 dramatically decreases. $\sigma_1(\omega)$ are small but do not vanish down to the lowest experimental frequency. The inset of figure 3 shows that the *dc* conductivity is also non-zero, and close to the extrapolated zero-frequency optical conductivity $\sigma_1(\omega \to 0)$ at 10 K. Therefore no energy gap opens in the low frequency range. Our data indicates that the negative $\mathrm{d}\rho/\mathrm{d}T(\mathrm{T})$ is not caused by an energy gap at Fermi level in the electric structure. This is consistent with nonzero electronic specific heat [6]. When frequency increases further to above 10 000 cm^{-1}, $\sigma_1(\omega)$ is almost frequency independent.

Figure 4 displays the real part of the dielectric constant $\epsilon_1(\omega)$. Similar to $\sigma_1(\omega)$, the real parts of the dielectric constants at all temperatures have the same typical characterizations. In a high frequency region $\epsilon_1(\omega)$ has a small positive value. With ω decreasing, $\epsilon_1(\omega)$ decreases and crosses the horizontal line at about 10 000 cm^{-1}. With ω decreasing further, ϵ_1 reaches a minimum at about 2000 cm^{-1}, then turns up, and becomes

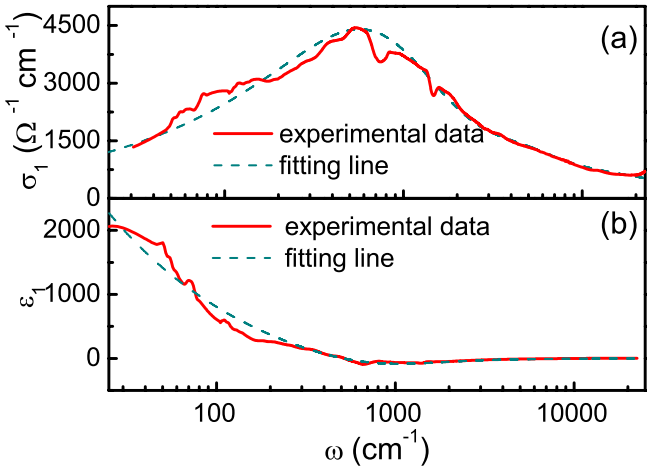

Figure 5. The fitting of the frequency dependence of (*a*) the optical conductivity $\sigma_1(\omega)$ and (*b*) the real part of the dielectric constant $\epsilon_1(\omega)$ at 100 K. The dashed lines are the fitting results for $\sigma_1(\omega)$ and $\epsilon_1(\omega)$, respectively.

positive below 550 cm^{-1}. It is noted that changes in $\sigma_1(\omega)$ are correlated with the changes in $\epsilon_1(\omega)$. Figures 5(*a*) and (*b*) are logarithmic scale plots of the real part of the optical conductivity $\sigma_1(\omega)$ and the real part of the dielectric constant $\epsilon_1(\omega)$ at 100 K to highlight the typical spectra details in the low frequency range. Between 550 cm^{-1} and 5000 cm^{-1}, both $\sigma_1(\omega)$ and $\epsilon_1(\omega)$ show a Drude type behavior. Below 550 cm^{-1} both of them greatly deviate from the Drude behaviour.

The peak structure of $\sigma_1(\omega)$ and positive $\epsilon_1(\omega)$ at low frequency suggest carrier localization in $BaOsO_3$. To support this picture, we use a localization modified Drude model (LMD) in the framework of the Anderson–Mott localization theory to reproduce the spectral structure in $\sigma_1(\omega)$ and $\epsilon_1(\omega)$ [15–18] ,

$$\sigma_{\mathrm{LMD}}(\omega) = \frac{\omega_p^2}{4\pi}\frac{\tau}{(1+\omega^2\tau^2)}\Big[1 - \frac{C}{(k_{\mathrm{F}}\upsilon_{\mathrm{F}})^2\tau^2} + \frac{C}{(k_{\mathrm{F}}\upsilon_{\mathrm{F}})^2\tau^{3/2}}(3\omega)^{1/2}\Big] \quad (1)$$

$$\epsilon_{\mathrm{LMD}}(\omega) = \varepsilon_\infty + \frac{\omega_p^2\tau^2}{(1+\omega^2\tau^2)}\Big[\frac{C}{(k_{\mathrm{F}}\upsilon_{\mathrm{F}})^2\tau^2}\Big(\sqrt{\frac{3}{\omega\tau}} - (\sqrt{6}-1)\Big) - 1\Big] \quad (2)$$

where ω_p is the plasma frequency, k_{F} is the Fermi wave vector, υ_{F} is the Fermi velocity, τ is the relaxation time, ϵ_∞ is the high energy dielectric constant, and C is a universal constant ($\sim$1). According to the electronic structure calculation [13], the Os 5d band splits into Os 5d t_{2g} and e_g bands in the OsO_6 octahedral crystal field. The Os 5d t_{2g} bands hybridize with O 2p bands, and locate in the range of -9.0 to 0.5 eV. The bands above 0.5 eV are the Os e_g manifold. The main density of state (DOS) in the energy range of -3.0 to +4.0 eV is contributed by the Os 5d bands and the O 2p bands. Our experiment was performed up to 25 000 cm^{-1} which is in this range. To fit the conductivity spectra very well, we need to add two interband transition peaks at high frequencies. Then, the total real part

Table 1. The parameters of equations (1) and (3) at 300 K, 100 K and 10 K.

T (K)	10	100	300
ω_p (cm^{-1})	16 190	16 190	16 000
τ ($\times 10^{-14}$ s)	3.30	3.40	2.90
$k_F\lambda$	0.98	1.01	0.96
T (K)	10	100	300
$\omega_{p,1}$ (cm^{-1})	16 000	15 000	15 200
$\omega_{0,1}$ (cm^{-1})	4770	4770	4770
γ_1 (cm^{-1})	7000	7000	7200
$\omega_{p,2}$ (cm^{-1})	32 500	32 500	33 500
$\omega_{0,2}$ (cm^{-1})	16 300	16 300	16 300
γ_2 (cm^{-1})	43 000	41 000	40 000

of conductivity can be written as:

$$\sigma_1 = \sigma_{\mathrm{LMD}} + \Sigma \frac{\omega_{p,i}^2}{4\pi} \frac{\omega^2 \gamma_i}{(\omega^2 - \omega_{0i}^2)^2 + \gamma_i^2 \omega^2} \tag{3}$$

where $\omega_{p,i} (i = 1, 2)$ are the strengths of the bounded carriers associated with the Lorentz component and $\gamma_i (i = 1, 2)$ are the damping coefficients. We find that the spectra could be well reproduced at all temperatures. As an example, figure 5 shows the typical $\sigma_1(\omega)$ (a) and the real part of the dielectric constant $\epsilon_1(\omega)$ (b) experimental data at 100 K and the fitting results using the same fitting parameters. The fitting parameters are listed in table 1. In general, peaks of 4770 cm^{-1} (about 0.6 eV) and 16 300 cm^{-1}(about 2.0 eV) observed in figure 5 could be attributed to the interband transitions from the occupied Os 5d t_{2g} states being hybridized with O 2p states, to the unoccupied part of the Os 5d e_g states. The localization modified itinerant carriers have an average life time of about 3×10^{-14} s. It varies slightly when T drops from 300 K to 10 K, while the longest life time is at 100 K. These values are about one order of magnitude lower than those of metals($\tau > 10^{-13}$ s). We could calculate $k_F\lambda$ from the ordering parameters $\tau k_F \upsilon_F / C$, using $\lambda = \tau \upsilon_F$($\lambda$ is the mean free path). As listed in table 1, for all temperatures $k_F\lambda$ are close to the Ioffe–Regel criterion $k_F\lambda \sim 1$, indicating that the system is at the boundary of a metal-insulator (MI) transition.

We noticed that the reflectivity and optical conductivity spectra vary with temperature (figures 2 and 3) up to a very high frequency. It is well known that the spectral weight of the optical conductivity gives a measure of the effective carrier number and obeys the f-sum rule:$\int_0^\infty \sigma_1(\omega)\mathrm{d}\omega = \pi n e^2/2m_0$, where n is the total electron density in the material, e is the electronic charge and m_o is the free electron mass. Figure 6 is the ω dependence of the spectral weight of $\sigma_1(\omega)$ given by $\mathrm{SW}(\omega_c) = \int_0^{\omega_c} \sigma_1(\omega)\mathrm{d}\omega$, where ω_c is a cutoff frequency. The sum rule is not obeyed until the frequency is up to 2.25 eV. The energy scale is about half of the theoretical band width in the first-principles calculation including SOC interaction. The spectral weight redistribution over a large energy scale may indicate the presence of the relatively strong correlation effect. Actually, such a behaviour has been observed in other 4d correlated localization systems [19–21], for example $SrTi_{1-x}Ru_xO_3$, Sr_2RuO_4. All the above behaviours suggest that the system sits at the boundary of the MIT and the electrons are correlated and localized.

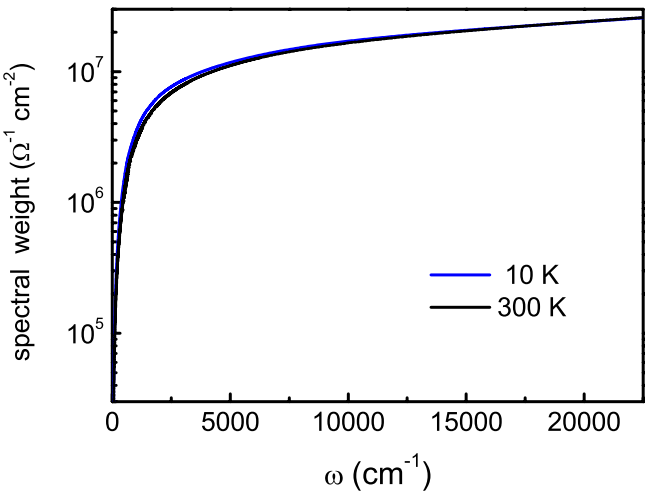

Figure 6. The spectral weight of the optical conductivity at 10 K and 300 K.

4. Conclusion

We report on our optical reflectance investigations on cubic perovskite $BaOsO_3$. No energy gap is observed in the far infrared region with temperature decreasing in the optical measurements. The localized response of the real part of the optical conductivity of the electrons near the Fermi surface is observed at all experimental temperatures. The localization modified Drude model is used to fit the optical response of the conducting carriers and obtain their life time. Along with the temperature decreasing, the life time of the itinerant carriers increases at first, then decreases. The fact that $k_F\lambda$ is close to the Ioffe–Regel criterion $k_F\lambda \sim 1$ indicates that the system is at the boundary of the metal-insulator transition. Large-energy-scale redistribution of the spectral weight is observed. Our observations and analysis show that the electrons near the Fermi surface are localized in $BaOsO_3$.

Acknowledgments

This work is supported by the 973 project of the Ministry of Science and Technology of China (No. 2011CB921701, No. 2011CBA00110, No. 2010CB923001), the National Science Foundation of China (11120101003), the Funding Program for World Leading Innovative R&D on Science and Technology (FIRST Program) of Japan, and the Grant-in-Aid for Scientific Research No. 22246083 from JSPS. We acknowledge the helpful discussions with Professor X Dai and Professor J L Luo.

References

[1] Kim B J *et al* 2008 *Phys. Rev. Lett.* **101** 076402
[2] Kim B J, Ohsumi H, Komesu T, Sakai S, Morita T, Takagi H and Arima T 2009 *Science* **323** 1329
[3] Ishii K, Jarrige I, Yoshida M, Ikeuchi K, Mizuki J, Ohashi K, Takayama T, Matsuno J and Takagi H 2011 *Phys. Rev.* B **83** 115121
[4] Padilla W J, Mandrus D and Basov D N 2002 *Phys. Rev.* B **66** 035120
[5] Reading J, Knee C S and Weller M T 2002 *J. Mater. Chem.* **12** 2376

[6] Shi Y G *et al* 2013 *J. Am. Chem. Soc.* **135** 16507
[7] Bremholm M, Dutton S, Stephens P and Cava R 2011 *J. Solid State Chem.* **184** 601
[8] Mandrus D, Thompson J R, Gaal R, Forro L, Bryan J C, Chakoumakos B C, Woods L M, Sales B C, Fishman R S and Keppens V 2001 *Phys. Rev.* B **63** 195104
[9] Ryden W D, Lawson A W and Sartain C C 1969 *Phys. Rev.* B **1** 1494
[10] Du L, Sheng X L, Weng H M and Dai X 2013 *Europhys. Lett.* **101** 27003
[11] Du L, Dai X and Huang L 2013 *Eur. Phys. J.* B **86** 94
[12] Pesin D and Balents L 2010 *Nat. Phys.* **6** 376
[13] Jung M C and Lee K W 2014 *Phys. Rev.* B **90** 045120
[14] Ruvalds J and Virosztek A 1991 *Phys. Rev.* B **43** 5498
[15] Li G, Zheng P, Wang N L, Long Y Z, Chen Z J, Li J C and Wan M X 2004 *J. Phys.: Condens. Matter* **63** 6195
[16] Martens H C F, Reedijk J A, Brom H B, de Leeuw D M and Menon R 2001 *Phys. Rev.* B **63** 073203
[17] Romijin I G, Hupkes H J, Martens H C F, Brom H B, Mukherjee A K and Menon R 2003 *Phys. Rev. Lett.* **90** 176602
[18] Kittel C 1976 *Introduction to Solid State Physics* (New York: Wiley)
[19] Kim K W, J S Lee, Noh T W, Lee S R and Char K 2005 *Phys. Rev.* B **71** 125104
[20] Pucher K *et al* 2002 *Phys. Rev.* B **65** 104523
[21] Katsufuji T, Kasai M and Tokura Y 1996 *Phys. Rev. Lett.* **76** 126